The Journal of Immunology

RESEARCH ARTICLE | MARCH 20 2023

A Small Molecule RIG-I Agonist Serves as an Adjuvant to Induce Broad Multifaceted Influenza Virus Vaccine Immunity FREE

Emily A. Hemann; ... et. al

J Immunol (2023) 210 (9): 1247–1256.
https://doi.org/10.4049/jimmunol.2300026

A Small Molecule RIG-I Agonist Serves as an Adjuvant to Induce Broad Multifaceted Influenza Virus Vaccine Immunity

Emily A. Hemann,*,† Megan L. Knoll,* Courtney R. Wilkins,*,[1] Caroline Subra,‡ Richard Green,* Adolfo García-Sastre,§,¶,‖ Paul G. Thomas,# Lydie Trautmann,‡, Renee C. Ireton,* Yueh-Ming Loo,*,[2] and Michael Gale, Jr.***

Retinoic acid–inducible gene I (RIG-I) is essential for activating host cell innate immunity to regulate the immune response against many RNA viruses. We previously identified that a small molecule compound, KIN1148, led to the activation of IFN regulatory factor 3 (IRF3) and served to enhance protection against influenza A virus (IAV) A/California/04/2009 infection. We have now determined direct binding of KIN1148 to RIG-I to drive expression of IFN regulatory factor 3 and NF-κB target genes, including specific immunomodulatory cytokines and chemokines. Intriguingly, KIN1148 does not lead to ATPase activity or compete with ATP for binding but activates RIG-I to induce antiviral gene expression programs distinct from type I IFN treatment. When administered in combination with a vaccine against IAV, KIN1148 induces both neutralizing Ab and IAV-specific T cell responses compared with vaccination alone, which induces comparatively poor responses. This robust KIN1148-adjuvanted immune response protects mice from lethal A/California/04/2009 and H5N1 IAV challenge. Importantly, KIN1148 also augments human CD8$^+$ T cell activation. Thus, we have identified a small molecule RIG-I agonist that serves as an effective adjuvant in inducing noncanonical RIG-I activation for induction of innate immune programs that enhance adaptive immune protection of antiviral vaccination. ***The Journal of Immunology*****, 2023, 210: 1247–1256.**

Non–self-detection of pathogen-associated molecular patterns (PAMPs) by specialized pattern recognition receptors initiates innate immune signaling cascades that result in tailored antimicrobial responses to limit infection. These responses include the production of cytokines, chemokines, and/or type I and II IFNs that mediate antiviral defense and regulate adaptive immune responses to clear infection and provide long-term memory protection (1, 2). Specifically, the pattern recognition receptor family of retinoic acid–inducible gene I (RIG-I)-like receptors (RLRs), RIG-I and melanoma differentiation–associated protein 5 (MDA5), is RNA helicases and members of the RLR family. RIG-I and MDA5 are essential for the initial detection of most RNA viruses, where they sense and bind to viral RNA in the cytosol of the host cell (3–5). On engaging its cognate PAMP, short dsRNA, or ssRNA

*Department of Immunology, Center for Innate Immunity and Immune Disease, University of Washington, Seattle, WA; †Department of Microbial Infection and Immunity, The Ohio State University, Columbus, OH; ‡The Henry M. Jackson Foundation for the Advancement of Military Medicine and the U.S. Military HIV Research Program, Bethesda, MD; §Department of Microbiology, The Tisch Cancer Institute, Global Health and Emerging Pathogens Institute, Icahn School of Medicine at Mount Sinai, New York, NY; ¶Division of Infectious Diseases, Department of Medicine, The Tisch Cancer Institute, Global Health and Emerging Pathogens Institute, Icahn School of Medicine at Mount Sinai, New York, NY; ‖Department of Pathology, Molecular and Cell-Based Medicine, The Tisch Cancer Institute, Global Health and Emerging Pathogens Institute, Icahn School of Medicine at Mount Sinai, New York, NY; #Department of Immunology, St. Jude Children's Research Hospital, Memphis, TN; and **Vaccine and Gene Therapy Institute, Oregon Health & Science University, Beaverton, OR

[1]Current address: Adaptive Biotechnologies, Seattle, WA.

[2]Current address: Vaccine and Immune Therapies, BioPharmaceuticals R&D, AstraZeneca, Gaithersburg, MD.

ORCIDs: 0000-0002-6398-3492 (E.A.H.); 0000-0003-4001-7686 (C.R.W.); 0000-0001-5272-0972 (C.S.); 0000-0002-6551-1827 (A.G.-S.); 0000-0001-7955-0256 (P.G.T.); 0000-0002-3012-0009 (L.T.); 0000-0002-5844-9981 (R.C.I.); 0000-0002-6332-7436 (M.G.).

Received for publication January 9, 2023. Accepted for publication February 10, 2023.

This work was supported by the National Institute of Allergy and Infectious Diseases, National Institutes of Health grants and contracts (HHSN272200900035C, HHSN27220130023C, HSSN272201400055C, U01AI151698, and U19AI100625 Project 3 to M.G.; 5U01AI150747 to P.G.T.; 75N93019C00051, 75N93019C00046, and P01AI097092 to A.G.-S.; and K22AI146141 to E.A.H.). This work was also supported by a cooperative agreement (W81XWH-07-2-0067, W81XWH-11-2-0174, and W81XWH-18-2-0040) between the Henry M. Jackson Foundation for the Advancement of Military Medicine Inc. and the U.S. Department of Defense. In addition, this work was supported by the National Institutes of Health-funded St. Jude Center of Excellence for Influenza Research and Surveillance (HHSN272201400006C), ALSAC (P.G.T.), and the Center for Research on Influenza Pathogenesis and Transmission, a National Institute of Allergy and Infectious Diseases, National Institutes of Health–funded Center of Excellence for Influenza Research and Response contract (75N93021C00014 to A.G.-S.). E.A.H. was also supported by American Heart Association Postdoctoral Award 17POST33660907.

This project was initially conceived and directed by Y.-M.L. and M.G. R.C.I. served as project manager for all studies. E.A.H. and Y.-M.L. designed experiments and analyzed data. C.R.W. developed the computational pipelines and conducted bioinformatics analyses. R.G. conducted bioinformatics data analysis, visualization, and deposition. E.A.H. performed in vivo vaccination and challenge studies. C.S. performed the human T cell priming experiment with guidance from L.T., Y.-M.L., and M.L.K. performed the remaining studies. P.G.T. generated vaccine stocks, and A.G.-S. provided influenza virus strains. The manuscript was written by E.A.H. and edited by Y.-M.L., R.C.I., and M.G. All authors read and approved the final manuscript.

The microarray data presented in this article have been submitted to the National Center for Biotechnology Information Gene Expression Omnibus (https://www.ncbi.nlm.nih.gov/geo/query/acc.cgi?acc=GSE205964) under accession number GSE205964.

The content of this manuscript is solely the responsibility of the authors and does not necessarily represent the official views of any of the institutions mentioned, the U.S. Department of the Army, the U.S. Department of Defense, or the Henry M. Jackson Foundation for the Advancement of Military Medicine.

Address correspondence and reprint requests to Emily A. Hemann or Yueh-Ming Loo and Michael Gale, Jr., Ohio State University College of Medicine, 460 W 12th Avenue, 718 BRT, Columbus, OH 43210 (E.A.H.) or Department of Immunology, Center for Innate Immunity and Immune Disease, University of Washington, 750 Republican Street, Seattle, WA, 98109 (Y.-M.L. and M.G.). E-mail addresses: emily.hemann@osumc.edu (E.A.H.) or yueh-ming.loo@astrazeneca.com (Y.-M.L.) and mgale@uw.edu (M.G.)

The online version of this article contains supplemental material.

Abbreviations used in this article: CARD, caspase activation and recruitment domain; cDMEM, complete DMEM; DC, dendritic cell; GC, germinal center; HA, hemagglutinin; HAU, hemagglutinin unit; HCV, hepatitis C virus; H1N1, A/California/04/2009; IAV, influenza A virus; IAV-SV, influenza A virus split vaccine; IRF, IFN regulatory factor; MAVS, mitochondrial antiviral signaling adaptor; MDA, melanoma differentiation–associated protein; MEF, mouse embryonic fibroblast; NA, neuraminidase; NP, nucleoprotein; PAMP, pathogen-associated molecular pattern; PR8, A/Puerto Rico/8/1934; RD, repressor domain; RIG-I, retinoic acid–inducible gene I; RLR, retinoic acid–inducible gene I–like receptor; SeV, Sendai virus.

containing polyuridine motifs marked with 5′-triphosphates, RIG-I is released from its basal, autoinhibited state to initiate a signaling cascade that typically culminates in the induction of IFN regulatory factors (IRFs) 3/7– and NF-κB–dependent transcriptional programs (6–9). These transcriptional programs include expression of antiviral genes, proinflammatory cytokines, and IFNs that coordinately function to limit virus infection.

Many microbial PAMPs are effective vaccine adjuvants through their innate immune activation properties. For example, the TLR agonists CpG oligodeoxynucleotides (TLR9) and monophosphoryl lipid A (TLR4) are agonists of IRF3 or NF-κB actions in innate immune programming and are approved for use in vaccines for hepatitis B virus, herpes zoster, influenza virus, and papillomavirus (10, 11). These PAMP-derived adjuvants target specific, defined immune pathways to elicit their effects. Developing a broad arsenal of adjuvants that target different and specific arms of innate immunity, to be used independently or in combination, could allow for tailoring of the host immune response to individual vaccines for optimal protection against infection. Such a strategy may greatly enhance the efficacy of many subunit vaccines, such as those administered to protect against influenza virus infection, which exhibit lower immunogenicity as compared with live, attenuated, or inactivated vaccines. Indeed, several adjuvants are currently being investigated to reduce the amount of vaccine needed to provide protection (dose sparing), to elicit broader protection against viral variants not represented in the vaccine, or to enhance protection of immunocompromised populations (12–15). These strategies may be particularly useful in serving as an adjuvant for influenza virus vaccines against highly pathogenic avian influenza, where limited domestic supply and lack of inclusion in seasonal vaccine production limits availability in the event of a human transmission event and/or pandemic emergence.

Given the robust immune response induced downstream of RIG-I, synthetic PAMP RNAs that engage RIG-I and potently activate the host antiviral response are under development for therapies to control virus infection (16–21). These RIG-I–agonistic RNAs potentiate dendritic cell (DC) cross-presentation of Ag to CTLs and T follicular helper cell induction, leading to enhanced Ab production (17–20). When administered in combination with a vaccine, these RNAs improve protection of mice from subsequent influenza virus challenge. Similarly, we predicted that small molecules targeting the RIG-I pathway may induce innate immune programs that could serve as a vaccine adjuvant.

We previously conducted a cell-based screen in which we identified innate immune-activating small molecules that conferred either antiviral or adjuvant activities (22–24). KIN1000 and its medicinal chemistry optimized analogue KIN1148 belong to a class of benzobisthiazoles selected for further investigation because of their ability to activate IRF3 and enhance protection against A/California/04/2009 (H1N1) when administered in a prime-boost fashion (24). In this study, we demonstrate that KIN1148 directly engages RIG-I to activate IRF3- and NF-κB–dependent innate immune responses. Biochemical studies show that KIN1148 binds to RIG-I to drive RIG-I self-oligomerization and downstream signaling activation in an RNA- and ATP-independent manner, highlighting a previously undescribed mode of RIG-I activation induced by KIN1148. Transcriptional programs induced by KIN1148 treatment exhibit shared and unique signatures to that induced by other RIG-I agonists including Sendai virus (SeV) infection and hepatitis C virus (HCV) PAMP RNA transfection (7–9). KIN1148 adjuvants an influenza A virus (IAV) split vaccine (IAV-SV) at suboptimal dose to protect mice from lethal challenge with a recombinant highly pathogenic avian H5N1 influenza virus, A/Vietnam/1203/2004 hemagglutinin (HA) and neuraminidase (NA) combined with A/PR/8/34. When administered with H5 IAV-SV, KIN1148 enhanced both humoral and T cell immune responses to H5 IAV-SV. Importantly, ex vivo studies show that KIN1148 promoted DC maturation and Ag-dependent activation of human $CD8^+$ T cells, suggesting its potential efficacy as an adjuvant in humans. Thus, KIN1148 is a small molecule RIG-I agonist and, to our knowledge, a novel innate immune-inducing adjuvant.

Materials and Methods

Cells and viruses

The HEK293 and Madin–Darby canine kidney cell lines were maintained in complete DMEM (cDMEM), supplemented with 10% FBS, L-glutamine, sodium pyruvate, and nonessential amino acids. The THP-1 (human monocytic) cell line was maintained in complete RPMI (cRPMI), supplemented with 10% heat-inactivated FBS, L-glutamine, sodium pyruvate, and nonessential amino acids. THP-1 cells were differentiated in cRPMI supplemented with 40 nM PMA for 30 h before being used in experiments. Human PBMCs or monocytes were isolated from buffy coat of healthy human donors (Biological Specialty) by density centrifugation in Ficoll-Paque PLUS (GE Healthcare Life Sciences). Monocytes were enriched either through positive selection using CD14 MicroBeads (Miltenyi Biotech) or by adherence to tissue culture-treated plates. Monocytes were cultured in cRPMI supplemented with recombinant human IL-4 and GM-CSF (PeproTech) to generate immature monocyte-derived DCs, or cDMEM supplemented with recombinant human M-CSF (PeproTech) to generate macrophages. Bone marrow cells isolated from the bones of adult C57BL/6J mice were differentiated into bone marrow–derived macrophages in cDMEM supplemented with recombinant mouse M-CSF (PeproTech) or into bone marrow–derived DCs in cRPMI supplemented with recombinant mouse IL-4 and GM-CSF (PeproTech). Influenza virus strains A/California/04/2009 (H1N1), A/VN/1203/04 H5N1 recombinant containing HA with an attenuating mutation in the polybasic cleavage site and NA from the H5N1 virus and all other segments from A/Puerto Rico/8/1934 (PR8), and other H5 recombinants (A/Egypt/N03072/10 and A/Barn Swallow/HK/D10-1161/2010) containing HA with an attenuating mutation in the polybasic cleavage site from the H5 virus and all other segments from PR8 were propagated in eggs and titered in Madin–Darby canine kidney cells using plaque assay as described previously described (25). SeV strain Cantell was obtained from Charles River Laboratories.

Compounds

Compounds were synthesized by Life Chemicals, solubilized in 100% DMSO, and kept frozen as 10 mM stocks. The compounds were stored in small aliquots to prevent multiple freeze-thaws and were stepwise diluted to reach the desired concentration in 0.5% (v/v) DMSO for all treatments. Liposomal formulation of KIN1148 for in vivo use was performed by InImmune.

Preparation of vaccine stocks for in vivo studies

Influenza virus A/Cal/04/09 and PR8/H5N1 split vaccine stocks were prepared as previously described (26, 27). HA viral protein content was verified by immunoblot and SDS-PAGE with Coomassie blue staining, using stocks of BSA of known concentration as standard. Western blots were also performed to ensure presence of HA and nucleoprotein (NP) proteins within the vaccine stocks.

In vivo vaccine studies

Adult C57BL/6J mice were purchased from Jackson Laboratories. For IAV challenge studies, mice were immunized once i.m. with H5-SV or H1-SV in combination with PBS, and KIN1148 in a lipid-based liposomal formulation or the liposomal formulation (vehicle) alone. The mice were challenged 30 d later with 5× LD_{50} homologous IAV strain PR8/H5N1 (160 PFU in 50 μl) or mouse-adapted A/Cal/04/09 (1250 PFU in 50 μl), administered via intranasal instillation in both nares (28). For morbidity studies, mice were monitored daily for changes in body weight and clinical scores. Murine clinical scores correspond to the following: 0 = healthy mouse (baseline); 1 = slightly ruffled fur and active; 2 = ruffled fur and active; 3 = ruffled fur and inactive without other obvious symptoms; 4 = ruffled fur, inactive, hunched sides, mild respiratory symptoms (rapid breathing) with or without other symptoms, and body condition score of 2+; 5 = ruffled fur, inactive, hunched sides, severe respiratory symptoms (ataxia, clicking sounds while breathing), and body condition score of 2; and 6 = moribund, body condition score of 2–, and 30% weight loss. Mice that were moribund and/or exhibited ≥30% weight loss after IAV infection were euthanized. Additional groups of mice

were harvested on day 5 postinfection to determine pulmonary virus titer by plaque assay. For experiments analyzing immune responses, C57BL/6J mice were immunized i.m. with H5-SV in combination with PBS (no adjuvant control), blank liposome (vehicle control), and KIN1148 formulated in liposome or PBS alone (no vaccine control). Mice were boosted on day 14 and harvested 5 d later for serum analysis of Ab responses ELISA, H5N1 hemagglutination inhibition, and germinal center (GC) B cell and IAV-specific T cell responses by flow cytometry. All animal handling and experiments were conducted using protocols approved by the University of Washington Institutional Animal Care and Use Committee.

Antibodies

The following primary Abs were used for immunoblot detection: rabbit anti–RIG-I (969, raised in rabbit against a RIG-I caspase activation and recruitment domain [CARD] peptide sequence) (29), rabbit anti-MDA5 (Enzo Life Sciences), rabbit anti-LGP2 (IBL-America), rabbit anti-DHX15 (Abcam), rabbit anti-TRIM25 (Cell Signaling), rabbit anti-inhibitor of the κB kinase-γ (Santa Cruz), rabbit anti–mitochondrial antiviral signaling adaptor (MAVS; Novus Biologicals), rabbit anti-IRF7 (Cell Signaling), rabbit anti-IRF3 (KINETA), rabbit anti-IRF3 phospho-serine 396 (Cell Signaling), rabbit or mouse anti-FLAG (Sigma), mouse anti-TANK-binding kinase 1 (Imgenex), mouse anti-GAPDH (Abcam), and mouse anti-actin (EMD Millipore). HRP-conjugated secondary Abs were obtained from Jackson ImmunoResearch. Alexa Fluor 488–conjugated secondary Abs were obtained from Thermo Fisher Scientific. Near-infrared fluorescent dye (IRDye)-conjugated secondary Abs were obtained from LI-COR. The following fluorochrome-conjugated anti-mouse Abs were used for flow cytometry analysis: CD4 (BioLegend), CD8 (BioLegend), CD19 (BioLegend), Peanut agglutinin (Vector Labs), CD3 (BioLegend), and CD45.2 (BioLegend). The following fluorochrome-conjugated anti-human Abs were purchased from BioLegend and used for flow cytometry analysis: CD11c, CD80, CD83, CD86, HLA-DR, CD3, and CD8. Live cells were discriminated using Fixable Viability Dye eFluor780 (eBioscience). Melan-A, NP_{366}, and NP_{311} tetramers were acquired from the National Institutes of Health Tetramer Core Facility.

Ab response quantification

ELISA to detect influenza-specific Abs. ELISA to detect IAV-specific IgG and IgG1 was performed as previously described (24). In brief, ELISA plates (Costar) were coated with UV-inactivated recombinant H5N1 virus. Dilutions of mouse serum after prime-boost as described in Fig. 3C were plated. Anti-mouse IgG and IgG1 conjugated to biotin (Southern Biotech), High Sensitivity Streptavidin-HRP (ThermoFisher), and 1-Step Ultrafast TMB substrate (ThermoFisher) were used to detect Ab isotypes.

Hemagglutination inhibition assay. Hemagglutination inhibition assay was performed as previously described (30). In brief, dilutions of serum treated with receptor-destroying enzyme (Denkin-Seiken) are incubated with 160 HA units (HAUs)/ml influenza virus. Subsequently, this virus/serum mixture is incubated with 0.5% chicken RBCs (Rockland), and hemagglutination inhibition was measured after 30 min.

RT-PCR quantitation of innate immune genes

Cells were harvested in RLT lysis buffer (Qiagen), and total cellular RNA was purified using the RNeasy kit (Qiagen). cDNA was synthesized from the purified RNA by both random and oligo(dT) priming using the iScript cDNA synthesis kit (Bio-Rad). RNA levels were measured by the SYBR Green relative quantitation method using either a 7300 or Viia 7 RT-PCR machine (Applied Biosystems). Samples were normalized by subtracting the respective cycle threshold values of housekeeping genes GAPDH or human acidic ribosomal protein, and fold induction of specific genes was calculated relative to DMSO treatment control. Primer sequences are available on request.

Biotin-compound pulldown and immunoblot analyses

Cells were trypsinized and collected in radioimmunoprecipitation assay (RIPA) buffer (50 mM Tris-Cl [pH 7.5], 150 mM NaCl, 5 mM EDTA, 1% Nonidet P-40, 0.5% sodium deoxycholate, 0.1% SDS) supplemented with a mixture of protease inhibitors (Sigma) and phosphatase inhibitors (Calbiochem) and okadaic acid (Calbiochem). After cell lysis, nuclear material was removed by centrifugation at 15,000 × *g* for 10 min at 4°C. Cell lysates were quantified by bicinchoninic acid assay (Thermo Fisher Scientific), analyzed on a denaturing Tris-HCl polyacrylamide gel, and transferred onto nitrocellulose membranes. Cellular proteins of interest were detected by immunoblot analysis using specific primary Abs described earlier and secondary Abs conjugated to either HRP or near-infrared fluorescent dyes (IRDye; LI-COR). Immunoblots developed with HRP-conjugated secondary Abs were visualized by chemiluminescence on X-ray film and quantitated using the ImageJ software (see the National Institutes of Health ImageJ Web site at http://imagej.nih.gov/ij/ and Ref. 31). Immunoblots developed with IRDye-conjugated secondary Abs were captured and quantitated using the Odyssey CLx imaging system with Image Studio 5.x Software.

ATPase assay

ATPase assays were performed as previously described (23). In brief, 2 pmol RNA (unstimulatory negative control xRNA or stimulatory pU/UC RNA) was mixed with 5 pmol recombinant purified RIG-I and increasing concentrations of recombinant purified KIN1148 (0, 1.25, 2.5, 5, 10 pmol) (8). A total of 1 mM ATP (Sigma) was added and incubated for 15 min at 37°C. ATPase reaction buffer and BIOMOL Green (Enzo Life Sciences) were added to each sample and read at OD_{630} using a microplate reader.

Microarray analysis

Differentiated THP-1 cells were treated with small molecule compounds (KIN1000 and KIN1148 at 0.625, 2.5, or 10 μM), 25 IU/ml IFN-β diluted in cRPMI supplemented with 0.5% (v/v) DMSO, or treated with cRPMI supplemented with 0.5% (v/v) DMSO alone (DMSO). Control cells infected with 25 HAUs/ml SeV were maintained in cRPMI supplemented with 0.5% (v/v) DMSO after removal of the virus inoculum. Additional cells were transfected with 2 μg/ml polyU/UC RNA [RIG-I–specific PAMP RNA derived from the HCV genome (8)] or control XRNA [RNA segment derived from the HCV genome adjacent to and equivalent in length to polyU/UC that cannot induce RIG-I–dependent innate immune signaling (8)] using the *Trans*IT-mRNA Transfection kit (Mirus Bio). Cells were collected in RLT buffer (Qiagen) 20 h after treatment or infection. Total RNA purified using RNeasy kit (Qiagen) was submitted to Labcorp Seattle (previously Covance) for microarray analysis using Agilent SurePrint G3 Human Genome Microarrays (version 2). Array data were processed by the Gale laboratory using R (version 3.2.1)/Bioconductor (version 3.1) (see Web site by the R Development Core Team at https://www.r-project.org and Ref. 32). Raw data were quantile normalized followed by linear modeling using the limma package (version 3.24.15) (33). Differential gene expression was defined as at least a 2-fold change in expression with a Benjamini-Hochberg corrected $p < 0.01$ as compared with the appropriate negative control: xRNA transfection for polyU/UC, mock-infected cells for SeV, and DMSO for all other samples. The gene expression heatmap was clustered using Spearman correlation distances, and Gene Ontology Biological Processes enriched in lists of genes mapping to such clusters were determined using DAVID 6.7 (34, 35). Genes with predicted IRF7 binding sites according to the University of California at San Diego Genome Browser database were identified using Enrichr (36). Finally, genes mapping to the Reactome *Homo sapiens* IFN-α/β signaling pathway (R-HAS-909733) were identified using InnateDb (37). The microarray data discussed in this publication have been deposited in the NCBI Gene Expression Omnibus (38) and are accessible through Gene Expression Omnibus accession number GSE205964 (https://www.ncbi.nlm.nih.gov/geo/query/acc.cgi?acc=GSE205964).

DC maturation assay

Monocytes were separated from PBMCs of healthy individuals (Biological Specialty) using anti-CD14 magnetic beads. The monocytes were cultured in cRPMI supplemented with recombinant human IL-4 and GM-CSF (PeproTech) to induce DC differentiation. Days 6–7 immature monocyte-derived DCs are exposed for 16–18 h to cRPMI supplemented with small molecule compound (KIN1000 or KIN1148; at indicated doses) or 0.5 μg/ml LPS in a final concentration of 0.5% (v/v) DMSO, or cRPMI supplemented with a final concentration of 0.5% (v/v) DMSO alone. DCs were analyzed for expression of maturation markers on the cell surface by flow cytometry using an LSR II (BD Biosciences) and FlowJo v10.1 software (University of Washington Cell Analysis Facility).

Human ex vivo adjuvant assay

PBMCs from healthy HLA-A0201$^+$ individuals were cultured in Cell Gro DC medium (CellGenix) supplemented for GM-CSF and IL-4 to induce DC differentiation. After 24 h, Melan-A–HLA-A2 epitope peptide (39) in the presence of 40 ng/ml IFN-γ in combination with 0.5% (v/v) final concentration DMSO, 10 μM small molecule compound (KIN1000 or KIN1148), or 0.5 μg/ml LPS in a final concentration of 0.5% (v/v) DMSO was added to the culture medium. Twenty-four hours later and every 3 d, half of the media was replaced by fresh RPMI supplemented with human serum at a final concentration of 8% and IL-2. On day 11, the CD8$^+$ T cells frequency and absolute number specific for Melan-A/MART-1 were assessed by flow cytometry within the CD3$^+$CD8$^+$ T cell population using Melan-A–HLA-A2 tetramer staining.

Data analyses

Flow cytometry data were collected on a BD LSRII and analyzed with FlowJo v10. Statistical analyses were performed using GraphPad Prism 7 software

(GraphPad, La Jolla, CA). Depending on the number of variables and time points in each experiment, statistical analysis of mean differences between groups was performed by either a Student *t* test or a multiway ANOVA followed by a Bonferroni or Friedman post hoc analysis. Kaplan–Meier survival analyses were analyzed by the log-rank test. Specific statistical tests, *p* values, and sample size are indicated in the figure legends.

Results

KIN1148 is a small molecule agonist of IRF3 signaling that confers adjuvant activity

The cell-based screen that led to the discovery of KIN1000 (Fig. 1A) was intentionally designed for identification of IRF3 activating small molecules (22); the screen was conducted in Huh7 cells, a human hepatoma cell line in which RLR signaling to IRF3 is functional, whereas signaling through the cytosolic DNA-sensing pathway and the TLRs is defective (40–44). KIN1148 (Fig. 1A) was designed as a medicinal chemistry optimized analogue of KIN1000 (23, 24). KIN1148 treatment induces phosphorylation of IRF3 and NF-κB p65 (Fig. 1B), indicative of innate immune activation.

KIN1148 is a small molecule RIG-I agonist

To define cellular targets that may engage KIN1148 to mediate innate immune activation, we evaluated innate immune gene expression in mouse embryonic fibroblasts (MEFs) and human alveolar epithelial cells (A549) lacking specific RLRs. Specifically, we measured expression of *Ifit1*, an IRF3 target gene, and *Il6*, a proinflammatory cytokine NF-κB target gene. RIG-I–deficient cells demonstrate reduced innate immune gene expression (*Ifit1* and *Il6*) after KIN1148 treatment as compared with wild-type cells (Fig. 1C). KIN1148 induction of innate immune genes is similarly decreased in A549 cells lacking RIG-I as compared with control cells or MDA5-deficient cells (Supplemental Fig. 1A, 1B). Further, we found that biotin-tagged KIN1148 binds to RIG-I in a cell-free in vitro interaction, but the related RLRs MDA5 or LGP2 do not bind KIN1148 (Fig. 1D). Biotin-fluorescein (F in Fig. 1D) served as a small molecule negative control and did not bind any of the RLR proteins. In addition, biotin-KIN1148 does not bind directly to MAVS, the essential downstream RLR adaptor protein (Fig. 1D). Taken together, these data indicate that KIN1148 directly targets and binds to RIG-I. This interaction is further demonstrated by biotin-KIN1148 capture of endogenous RIG-I from whole-cell lysates prepared from HEK293 cells and MEFs (Supplemental Fig. 1C, 1D). Hence KIN1148 binds to both human and mouse RIG-I to induce innate immune activation.

On engaging PAMP RNA, RIG-I hydrolyzes ATP to undergo conformational change and initiate downstream signaling (45–47). We assessed the ability of KIN1148 to promote RIG-I hydrolysis of ATP by incubating purified recombinant RIG-I with DMSO or increasing concentrations of KIN1148 in the presence of ATP. KIN1148 alone does not lead to hydrolysis of ATP (Fig. 1E) despite the activation of IRF3 downstream of RIG-I when KIN1148 is added directly to cells (Fig. 1B). Interestingly, KIN1148 does not alter RIG-I ATPase activity when added in increasing amounts to either polyU/UC [a validated RIG-I PAMP RNA derived from the HCV genome (8)] or xRNA (an RNA of equivalent length from a region within the HCV genome adjacent to polyU/UC that does not activate RIG-I signaling) (Fig. 1E). Moreover, although KIN1148 competed with itself for biotin-KIN1148 capture of purified recombinant RIG-I, the addition of ATP or Adenylyl-imidodiphosphate did not compete for biotin-KIN1148 capture of RIG-I (Supplemental Fig. 1E).

The conformational change in RIG-I leads to the release of its tandem N-terminal CARDs from autoinhibition, which allows RIG-I to form homo-oligomers. RIPLET binds to oligomerized RIG-I, leading to ubiquitination and RIG-I translocation to intracellular membranes to interact with MAVS (48). This in turn triggers MAVS filamentation and recruitment of signaling cofactors to form an innate immune signalosome on MAVS that leads to innate immune activation (49–55). To define KIN1148 activation of RIG-I, we conducted biotin-KIN1148 pulldown assays using buffers of lower stringency to recover RIG-I plus associated factors from whole-cell lysates. Under such conditions, we recovered MAVS in addition to RIG-I from whole-cell lysates (Supplemental Fig. 1C). We additionally identified many of the cofactors that comprise the RIG-I signalosome and that are required for RIG-I signaling to the innate immune response (3, 5, 49, 50), including DHX15, TANK-binding kinase 1, TRIM25, NEMO or inhibitor of the κB kinase-γ, and IRF3 (Fig. 1F).

To determine where KIN1148 may bind to RIG-I, we investigated binding of biotin-KIN1148 with several RIG-I deletion mutants. Biotin-KIN1148 captured all RIG-I constructs that contain either the C-terminal repressor domain (RD) or the conserved DEAH helicase motifs, but not the construct that consists of the CARDs alone (Fig. 1G). The data suggest binding sites for KIN1148 are within the RD and the helicase domains of RIG-I, but not within the CARDs.

KIN1148 confers an innate immunity gene expression profile consistent with RIG-I activation

We next aimed to delineate the gene expression profiles of human macrophage-like THP-1 cells treated with KIN1148 or K1000 compared with cells treated with known innate immune agonists, including the TLR4 PAMP LPS and IFN-β for JAK/STAT-mediated signaling downstream of the IFN-α/β receptor. SeV-infected cells and polyU/UC RNA transfection served as controls for RIG-I– and MAVS-specific responses (Fig. 2).

We plotted all genes differentially expressed in at least one treatment by heatmap and performed hierarchical clustering using Spearman correlation as a distance measure (Fig. 2A). Patterns of gene expression across doses demonstrate KIN1148 induces changes in gene expression more potently than its parent KIN1000. Consistent with its role as a RIG-I agonist, KIN1148 promoted the expression of genes involved in the inflammatory response, defense response to virus, and a subset of genes involved in Ag processing and presentation. Many genes regulated by KIN1148 are also differentially expressed on polyU/UC transfection or SeV infection (Fig. 2B).

Further inspection of genes whose expression is perturbed by compound treatment demonstrates that KIN1148 induces the expression of many genes designated as "antigen presentation" (Fig. 2C) and "cytokines" (Fig. 2D) in a dose-dependent manner. Notably, KIN1148 treatment induces a cytokine expression profile that more closely resembles that induced by SeV infection, polyU/UC transfection, or LPS treatment as opposed to IFN-β treatment. Although the microarray included assessments of IFNA4, IFNA7, IFNA21, IFNB1, IFNW1, and IFNG, their expression was not detected after KIN1148 treatment (Supplemental Table I), whereas induction of IRF3 target genes was clearly represented. This outcome links KIN1148 binding to RIG-I with downstream IRF3 and NF-κB activation and induction of IRF3 and NF-κB target genes rather than a response attributed merely to induction of type I or type III IFNs. In summary, KIN1148 induces a gene expression profile that is consistent with RIG-I signaling activation in a manner of IRF3- and NF-κB–dependent activation that is distinct from IFN-induced responses.

KIN1148 augments protection against H5N1 and H1N1 and induces adaptive immune responses postvaccination

We next assessed KIN1148 for the ability to serve as an IAV-SV adjuvant. Reassortant A/PR/8/34 influenza viruses containing HA and NA from either A/Cal/04/09 (2009 pandemic H1N1 influenza virus [H1-SV]) or A/Vietnam/1203/2004 (PR8/H5N1 [H5-SV]) and all

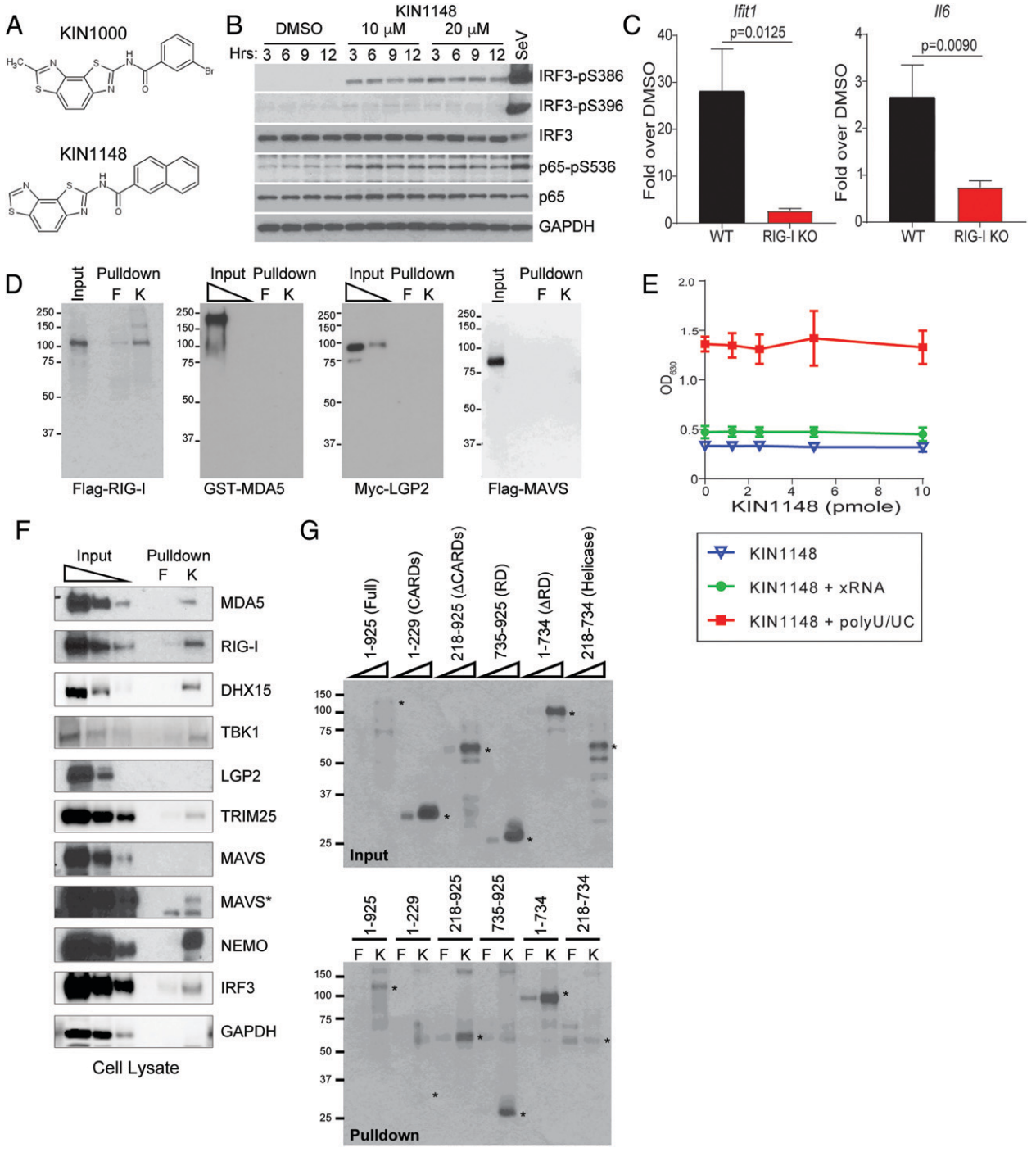

FIGURE 1. KIN1148 is a small molecule IRF3 and NF-κB agonist that binds to and induces RIG-I signaling activation. (**A**) Chemical structure of parent compound KIN1000 and its medicinal chemistry optimized lead KIN1148. (**B**) Western blot analysis of the phosphorylation state of IRF3 and NF-κB at time points up to 12 h after HEK293 cells were treated with KIN1148 at 10 or 20 μM. Included as comparison are cells treated with 0.5% DMSO (vehicle control) and cells infected with SeV at 40 HAUs/ml. (**C**) Quantitative RT-PCR analysis of *Ifit1* and *Il6* in wild-type and RIG-I$^{-/-}$ MEFs at 18 h after KIN1148 treatment as compared with respective DMSO controls. Fold induction over DMSO control from three independent experiments is shown. Error bars represent SD. (**D**) Western blot detection of input and pulldown products that associate with either biotin-fluorescein (F) or biotin-KIN1148 (K) beads using recombinant proteins generated using a rabbit reticulocyte lysate in vitro transcription and translation system and detected using Abs specific for the respective epitope tags. (**E**) BIOMOL green colorimetric analysis of free phosphate levels as an indication of RIG-I ATP hydrolysis activity. Purified recombinant RIG-I protein and ATP were incubated with DMSO or increasing concentrations of KIN1148 in the absence and presence of polyU/UC or xRNA. Each point shows the average concentration of free phosphates in each reaction from at least three independent experiments with error bars showing SD. (**F**) Western blot detection of endogenous RIG-I and associated signaling cofactors in the HEK293 whole-cell lysate (input) and among the pulldown products of biotin-KIN1148 beads (K) or biotin-fluorescein bead alone (F). MAVS* indicates higher exposure blot. (**G**) Western blot detection of various Flag-tagged RIG-I constructs generated by in vitro transcription and translation for interaction with biotin-fluorescein or biotin-KIN1148. Asterisks indicate expected location of band of interest across upper and lower blots in (G).

other genes from PR8 were inactivated to create vaccine stocks as previously described and confirmed to contain HA and NP proteins (26, 27). Mice were immunized i.m. with a suboptimal dose of H1-SV or H5-SV in combination with PBS, vehicle, or KIN1148 and challenged with 5× LD_{50} of homologous influenza virus (PR8/H5N1 or mouse-adapted A/Cal/04/09) 30 d postimmunization. Mice that

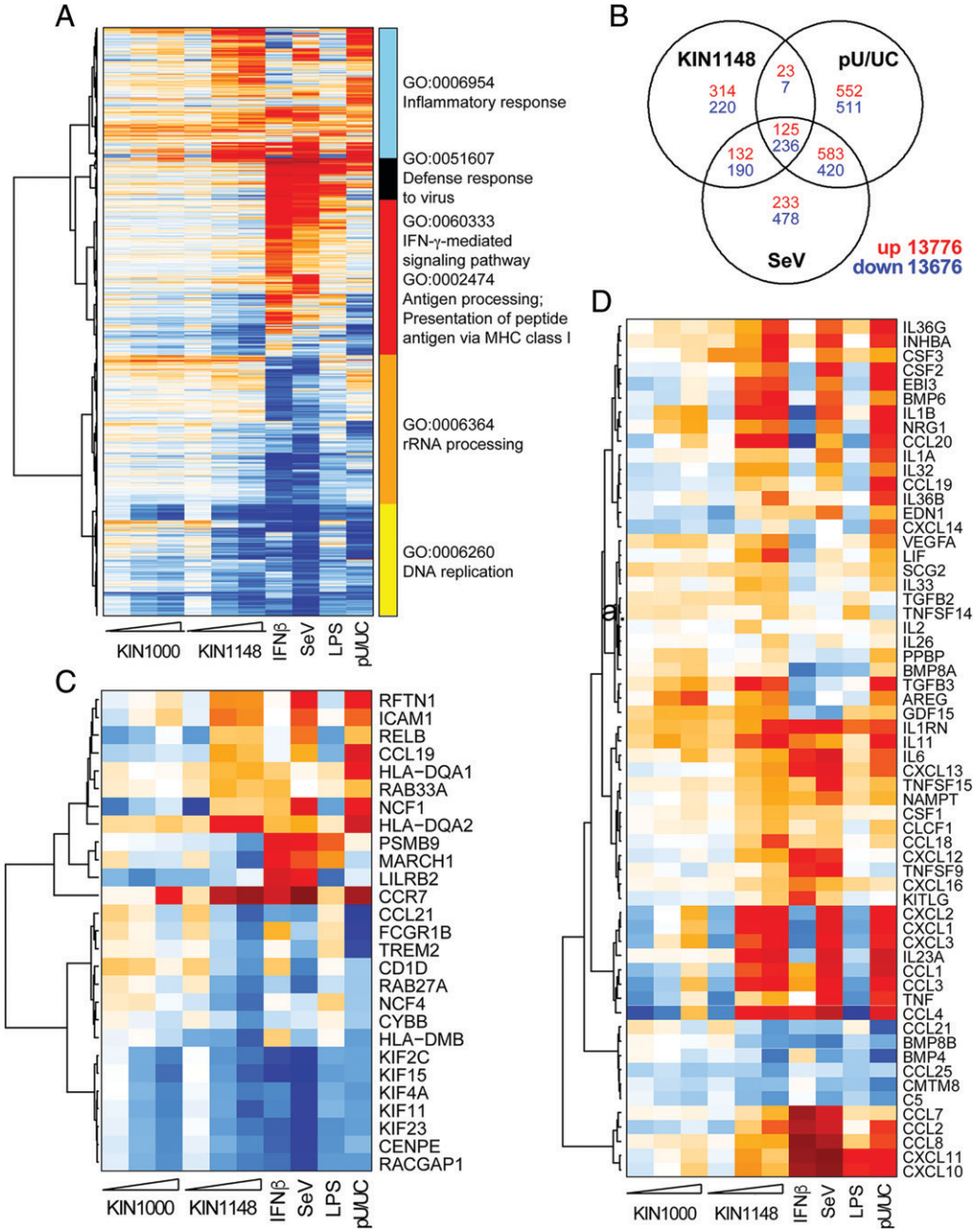

FIGURE 2. KIN1148 treatment induces a gene expression profile that shares common and unique properties to that achieved with LPS, SeV infection, and polyU/UC RNA transfection. Microarray analysis of THP-1 cells treated with KIN1000 or KIN1148 at concentrations up to 20 μM, 0.5 μg/ml LPS, or 100 IU/ml IFN-β as compared with DMSO control. For a RIG-I–specific gene expression signature, polyU/UC PAMP RNA-transfected cells were compared with those transfected with xRNA, whereas SeV-infected cells were compared with mock-infected cells. Differential gene expression is defined as at least a 2-fold change in expression with a Benjamini-Hochberg corrected $p < 0.01$ as compared with the respective negative controls. (**A**) Heatmap showing all genes differentially expressed in at least one treatment with hierarchical clustering and classification by the most highly enriched Gene Ontology (GO) biological process. (**B**) Venn diagram showing numbers of differentially expressed genes, up (red) and down (blue), that are shared and unique among cells stimulated with KIN1148, polyU/UC, or SeV. (**C** and **D**) Analysis showing global gene expression profile with Gene Ontology clustering of enriched genes. Heatmap of genes whose expression is perturbed by compound treatment and designated by gene clustering as (C) Ag presentation or (D) cytokines.

received IAV-SV in combination with KIN1148 showed significantly decreased mortality, reduced illness scores, and weight loss after lethal PR8/H5N1 (Fig. 3A) or lethal A/Cal/04/09 (Fig. 3B) challenge compared with IAV-SV + PBS or IAV-SV + vehicle control groups. This enhancement in survival is accompanied by a significant reduction in pulmonary virus titer on day 5 after challenge with A/Cal/04/09 (Fig. 3C). These data demonstrate that KIN1148 adjuvants H5-SV and H1-SV reduce pulmonary virus titer and protection on challenge.

To determine which protective immune responses were enhanced by KIN1148 in the context of IAV-SV to confer protection, we assessed serum Ab responses 5 d after D0/D14 i.m. prime-boost with H5-SV plus PBS, vehicle, or KIN1148. We observed a significant increase in total IgG and IgG1 in the serum of mice immunized with H5-SV + KIN1148 compared with immunization with PBS or vehicle (Fig. 3D). KIN1148 also significantly increased hemagglutination inhibition of homologous A/VN/1203/04, but also two other H5N1 recombinant strains, A/Egypt/N03072/10 PR8 recombinant and

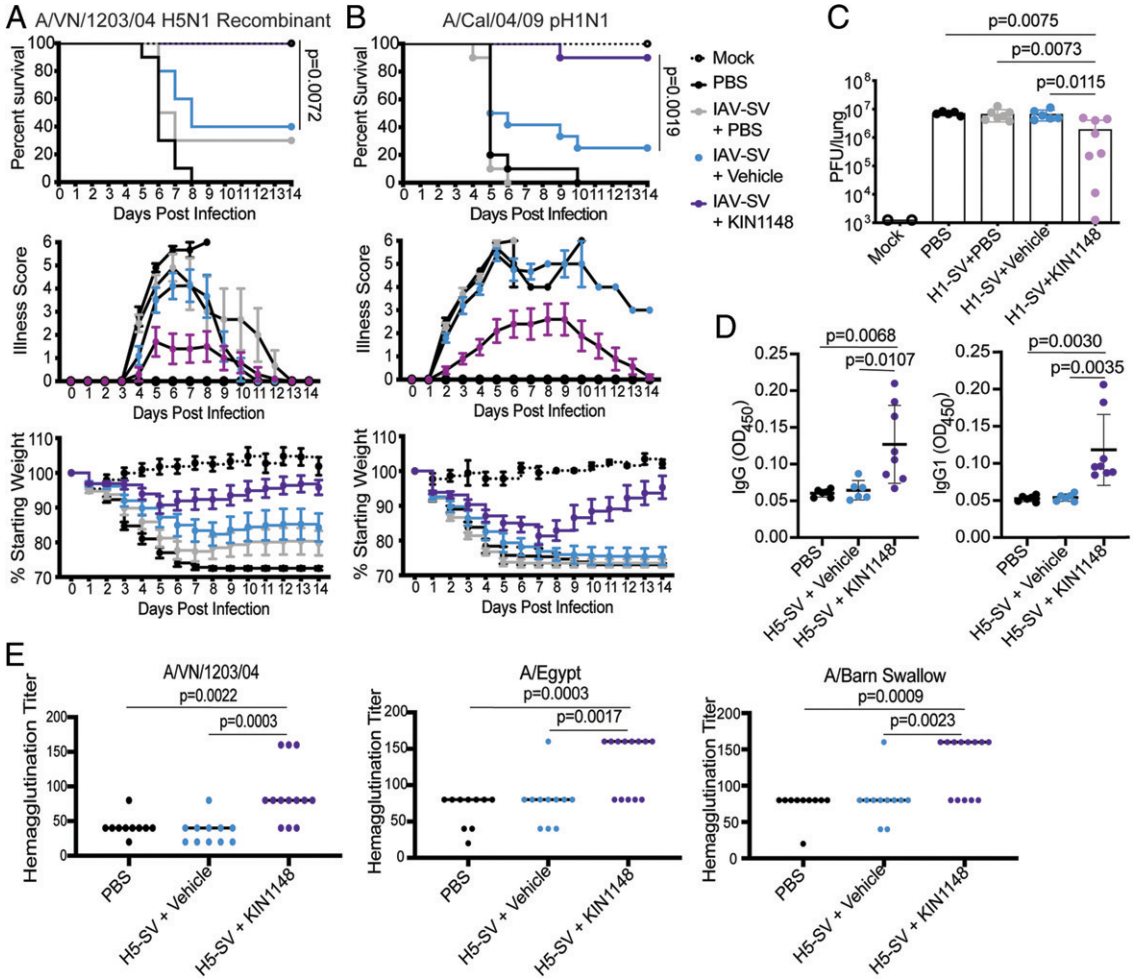

FIGURE 3. KIN1148 adjuvants for influenza virus vaccination induce humoral responses and confer protection against H1N1 and H5N1 infection. (**A–C**) C57BL/6J mice (n = 10 mice/group, except mock where n = 5) were immunized i.m. with (A) A/VN/1203/04 H5N1 6 + 2 SV (H5-SV) or (B) A/Cal/04/09 H1N1 SV (H1-SV) in combination with PBS (IAV-SV + PBS, gray circles), blank liposome (IAV-SV + vehicle, blue circles), KIN1148 formulated in liposome (IAV-SV + KIN1148, purple circles), or PBS alone (black circles). On day 30 postvaccination, mice were challenged intranasally with 5× LD_{50} of the homologous virus used for vaccination and monitored for survival (top), clinical illness (middle), and weight loss (bottom). (C) Mice were immunized and challenged as described in (A) using H1-SV. On day 5 postinfection, lungs were harvested, and virus titers were determined by plaque assay. n = 2 (mock) to 8 mice/group with data representative of two independent experiments. (**D**) C57BL/6J mice were immunized i.m. with PBS alone (PBS, black circles), H5-SV in combination with blank liposome (H5-SV + vehicle, blue circles), or H5-SV with KIN1148 formulated in liposomes (H5-SV + KIN1148, purple circles). Mice were boosted on day 14, and serum was collected 5 d later for analysis of A/VN/1203/04-specific Abs. n = 6–8 mice/group with data from two pooled experiments shown. (**E**) C57BL/6J mice were immunized as described in (D). Mice were administered a homologous boost on day 14, and serum was collected on day 19. The ability of Abs in the serum to prevent hemagglutination of homologous (A/VN/1203/04 H5N1 6 + 2) or heterologous (A/Egypt/N03072/10 H5 7 + 1, A/Barn Swallow/HK/D10-1161/2010 7 + 1) recombinant avian influenza viruses was determined. n = 10–13 mice/group with data from two pooled experiments shown.

A/Barn Swallow/HK/D10-1161/2010 PR8 recombinant (Fig. 3E). Together, these studies show KIN1148 serves as an adjuvant to induce broadly neutralizing Ab responses.

Given the ability of KIN1148 to serve as an adjuvant to enhance Ab responses in the context of IAV-SV, we assessed whether KIN1148 could augment cell-mediated immunity, potentially enhancing broad protection against IAV. Using the prime-boost strategy described for Fig. 4, we observed that KIN1148 significantly increases both the frequency and the numbers of GC B cells in the draining popliteal lymph node after vaccination with H5-SV (Fig. 4A). KIN1148 also significantly increased IAV-specific $CD4^+$ and $CD8^+$ T cell responses in the spleen after H5-SV vaccination (Fig. 4B, 4C). We observed similar results when A/Cal/04/09 SV was administered with KIN1148 (data not shown). Importantly, these data demonstrate that KIN1148 can augment H5-SV and H1-SV to induce broadly protective cellular immune responses typically not generated after vaccination with IAV-SV alone.

KIN1148 promotes human DC maturation and T cell maturation

To define mechanisms of KIN1148 adjuvant action in human immune cells, we evaluated its effects on DC maturation by treating human monocyte-derived DCs with DMSO, LPS, or KIN1148 for 18 h. KIN1148-treated cells exhibit greater cell surface expression of the DC costimulatory molecules CD83 and CD86 as compared with DMSO (Fig. 5A).

Given the ability of KIN1148 to lead to THP-1 gene responses associated with Ag presentation, induce costimulatory molecule upregulation of monocyte-derived DCs, and adjuvant H5-SV to induce IAV-specific $CD4^+$ and $CD8^+$ T cell responses in our murine model, we evaluated the ability of KIN1148 to enhance human Ag-specific

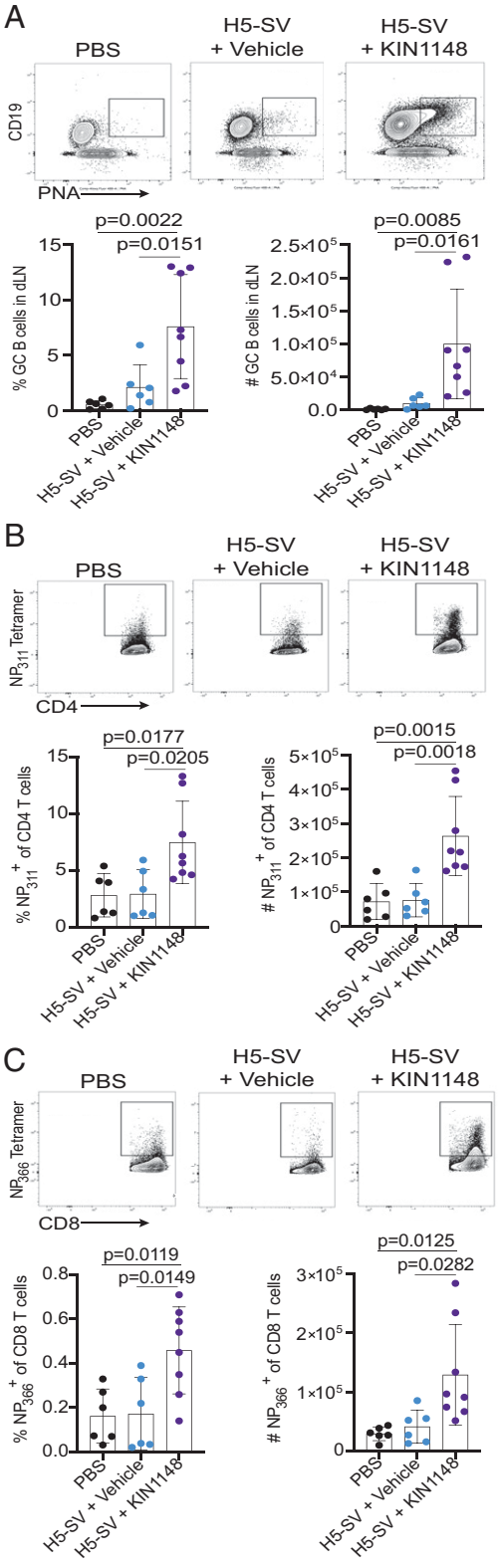

FIGURE 4. KIN1148 enhances cellular immune responses after H5N1 vaccination. C57BL/6J mice were immunized i.m. with PBS (black circles), H5-SV in combination with blank liposome (H5-SV + vehicle), or H5-SV with KIN1148 formulated in liposomes (H5-SV + KIN1148, purple circles). Mice were administered a homologous boost on day 14, and lung-draining lymph nodes (dLNs) and spleen were collected on day 19. (**A**) The frequency and number of Peanut agglutinin$^+$ GC B cells in dLN were determined by flow cytometry. (**B**) IAV-specific CD4$^+$ T cell responses were assessed by flow cytometry. (**C**) IAV-specific CD8$^+$ T cell responses were assessed by flow cytometry. n = 6–8 mice/group with data from two pooled experiments shown.

CD8$^+$ T cell responses. To simulate conditions similar to prime immunization ex vivo, we evaluated CD8$^+$ T cell responses to the Melan-A protein using PBMCs from healthy donors. The precursor frequency against this Ag is relatively high in HLA-A0201$^+$ individuals and has been shown to represent a normal naive CD8$^+$ T cell population in healthy individuals (56–58), allowing for testing of KIN1148 to augment CD8$^+$ T cell activation. PBMCs were pulsed with a Melan-A/MART-1 peptide in combination with DMSO, IFN-γ with DMSO, or IFN-γ with KIN1148 and cultured for 11 d. As anticipated, Melan-A/MART-1–specific CD8$^+$ T cell numbers represent a measurable fraction of total CD8$^+$ T cells after Melan-A/MART-1 peptide stimulation with or without IFN-γ (Fig. 5B). This population was significantly increased after coculture with PBMCs pulsed with Melan-A/MART-1 peptide in combination with KIN1148 + IFN-γ as compared with DMSO or DMSO + IFN-γ controls (Fig. 5B). Taken together, our data indicate that KIN1148 promotes Ag presentation leading to greater activation of naive human CD8$^+$ T cells.

Discussion

We report in this article the identification of KIN1148, a benzobisthiazole small molecule RIG-I agonist that induces IRF3- and NF-κB–dependent innate immune activation to confer adjuvant activity. KIN1148 was designed through structural–activity relationship studies to have improved solubility and pharmacokinetic properties compared with KIN1000, an IRF3-activating small molecule compound identified through screening (23).

Our results demonstrate that KIN1148 directly interacts with RIG-I in biochemical assays and cells, and signals for innate immune gene induction in a RIG-I–dependent manner. KIN1148 induces a pattern of gene expression resembling infection with SeV (an RNA virus that activates RIG-I) and by transfection of polyU/UC (a RIG-I–specific RNA agonist). However, we propose that KIN1148 interacts with RIG-I distinct from PAMP RNA, which binds to the RIG-I RD to induce conformational changes that release its CARDs to interact with downstream signaling cofactors. Our data demonstrate that KIN1148 binds not only RD but also the helicase domain of RIG-I. Our studies further reveal that KIN1148 does not compete with ATP or Adenylyl-imidodiphosphate for binding and does not lead to independent ATP hydrolysis despite signalosome formation and induction of gene responses with cellular treatment of KIN1148 alone. Together, this suggests, to our knowledge, a potentially novel mechanism for noncanonical RIG-I activation and highlights the potential usefulness of KIN1148 as an adjuvant. It is also possible that KIN1148 may direct signaling via additional cellular targets, but initial screens for these compounds were conducted in cells lacking functional TLRs and cytosolic DNA pathways to avoid other canonical virus-sensing pathways (40–44). Future studies will be needed to determine whether KIN1148 targets other immune pathways aside from the RLRs, TLRs, and cytosolic DNA-sensing pathways.

KIN1148 enhances the protection of mice from subsequent analogous challenge by a highly pathogenic H5N1 or pandemic H1N1 influenza virus beyond vaccine alone administered at a suboptimal dose. This vaccine dose-sparing effect alone is significant in that it could lead to greater availability of limited vaccine doses against highly pathogenic avian influenza should an outbreak occur in the human population. In addition, KIN1148 administered with H5 IAV-SV led to Ab responses able to neutralize other recombinant H5N1 influenza viruses, suggesting KIN1148 broadens vaccine-mediated protection against IAV strains not specifically included in the vaccination. Future studies will investigate this possibility of KIN1148 to broaden protection from heterosubtypic IAV challenge after vaccination.

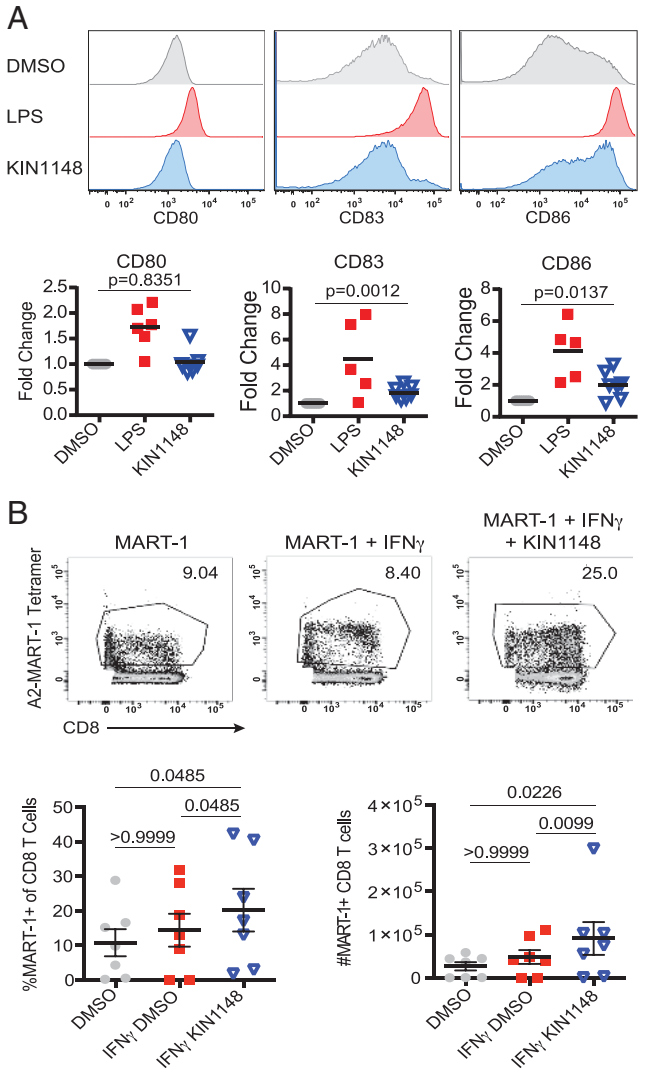

FIGURE 5. KIN1148 promotes DC maturation and human T cell proliferation. (**A**) Flow cytometry analysis of maturation markers expressed on the cell surface of human monocytic DCs after 18-h treatment with DMSO, LPS, or KIN1148. Histograms (top) of CD80, CD83, and CD86 on human monocytic DCs from a representative experiment. Graphs (bottom) showing the expression of each maturation marker from at least six different healthy donors, expressed as fold change in mean fluorescence intensity (MFI) as compared with DMSO control. (**B**) PBMCs from healthy HLA-A0201$^+$ donors were pulsed with Melan-A/MART-1 peptide in combination with DMSO or KIN1148 in the presence of IFN-γ for 24 h and then removed from the treatments to be cocultured with autologous T cells in the presence of IL-2. Cells were collected 11 d later and analyzed by flow cytometry for CD8$^+$ T cells that stain positive with the corresponding Melan-A/MART-1 tetramer. Density plot from a representative experiment showing CD8 and MART-1 tetramer staining and gating strategy (top). Graphs (bottom) showing the frequency and numbers of MART-1 tetramer$^+$ CD8$^+$ T cells from seven donors.

Previous studies have shown that the addition of RIG-I–activating RNA to vaccines, including pieces of viral RNA and synthetic polyI:C, can enhance the protection of mice compared with vaccine alone by leading to Th2-biased responses and enhancement of virus-specific Ab responses (17, 24). Importantly, our results demonstrate that KIN1148 promotes Ag-specific T cell responses in vivo in mice and ex vivo in humans. Because administration of H5 IAV-SV alone does not typically induce T cell–mediated immunity, our results suggest that KIN1148 serve to adjuvant vaccine-mediated protection in a way that broadens immunity against heterosubtypic or drifted IAV strains. Mechanistically, our ex vivo studies further demonstrate that KIN1148 promotes DCs maturation and their secretion of cytokines that functionally leads to the recruitment of a variety of immune cells.

Overall, this study reveals that a small molecule compound, KIN1148, directly binds to RIG-I in a noncanonical fashion, leading to IRF3 and NF-κB activation, DC activation and maturation, and enhanced Ag-specific T cell activation in vivo in mice and in human primary cells. KIN1148 in a liposomal formulation not only adjuvants protection in a murine model of H5N1 and pH1N1 infection but leads to the enhancement of cross-protective Ab responses and T cell responses known to provide broad protection against IAV.

Acknowledgments

We thank Jeffrey Posakony (Kineta, Inc.) for synthesizing biotinylated-KIN1148 and Ran Dong (University of Washington) for providing excellent technical support. Special thanks go to Kristin Bedard, Peter Probst, and Shawn Iadonato from Kineta, Inc. for providing KIN1000 and KIN1148, as well as valuable scientific discussions. We thank Drs. Alison M. Kell (University of New Mexico) and Jacob Yount (Ohio State University) for insightful feedback during preparation of this manuscript. We thank the National Institutes of Health Tetramer Core Facility (contract 75N93020D00005) for providing HLA-A2/MART-1 class I monomers, NP_{366} tetramers, and NP_{311} tetramers. This research was additionally supported by the Cell Analysis Facility Flow Cytometry and Imaging Core and the Center for Innate Immunity and Immune Disease at the University of Washington.

Disclosures

Y.-M.L. and M.G. are co-inventors on U.S. patent #9,775,894 entitled "Methods and compositions for activation of innate immune responses through RIG-I like receptor signaling" issued October 3, 2017. Kineta Inc. owns the patent and licensing rights for KIN1000 and KIN1148. The A.G.-S. laboratory has received research support from Pfizer, Senhwa Biosciences, Kenall Manufacturing, Avimex, Johnson & Johnson, Dynavax, 7Hills Pharma, Pharmamar, ImmunityBio, Accurius, Nanocomposix, Hexamer, N-fold LLC, Model Medicines, Atea Pharma, Applied Biological Laboratories, and Merck, outside of the reported work. A.G.-S. has consulting agreements for the following companies involving cash and/or stock: Vivaldi Biosciences, Contrafect, 7Hills Pharma, Avimex, Vaxalto, Pagoda, Accurius, Esperovax, Farmak, Applied Biological Laboratories, Pharmamar, Paratus, CureLab Oncology, CureLab Veterinary, Synairgen, and Pfizer, outside of the reported work. A.G.-S. is inventor on patents and patent applications on the use of antivirals and vaccines for the treatment and prevention of virus infections and cancer, owned by the Icahn School of Medicine at Mount Sinai, New York, outside of the reported work.

References

1. Brubaker, S. W., K. S. Bonham, I. Zanoni, and J. C. Kagan. 2015. Innate immune pattern recognition: a cell biological perspective. *Annu. Rev. Immunol.* 33: 257–290.
2. Cui, J., Y. Chen, H. Y. Wang, and R. F. Wang. 2014. Mechanisms and pathways of innate immune activation and regulation in health and cancer. *Hum. Vaccin. Immunother.* 10: 3270–3285.
3. Kell, A. M., and M. Gale, Jr. 2015. RIG-I in RNA virus recognition. *Virology* 479–480: 110–121.
4. Loo, Y. M., and M. Gale, Jr. 2011. Immune signaling by RIG-I-like receptors. *Immunity* 34: 680–692.
5. Chan, Y. K., and M. U. Gack. 2015. RIG-I-like receptor regulation in virus infection and immunity. *Curr. Opin. Virol.* 12: 7–14.
6. Kato, H., O. Takeuchi, E. Mikamo-Satoh, R. Hirai, T. Kawai, K. Matsushita, A. Hiiragi, T. S. Dermody, T. Fujita, and S. Akira. 2008. Length-dependent recognition of double-stranded ribonucleic acids by retinoic acid-inducible gene-I and melanoma differentiation-associated gene 5. *J. Exp. Med.* 205: 1601–1610.
7. Kell, A., M. Stoddard, H. Li, J. Marcotrigiano, G. M. Shaw, and M. Gale, Jr. 2015. Pathogen-associated molecular pattern recognition of hepatitis C virus transmitted/founder variants by RIG-I is dependent on U-core length. *J. Virol.* 89: 11056–11068.

8. Saito, T., D. M. Owen, F. Jiang, J. Marcotrigiano, and M. Gale, Jr. 2008. Innate immunity induced by composition-dependent RIG-I recognition of hepatitis C virus RNA. *Nature* 454: 523–527.
9. Schnell, G., Y. M. Loo, J. Marcotrigiano, and M. Gale, Jr. 2012. Uridine composition of the poly-U/UC tract of HCV RNA defines non-self recognition by RIG-I. *PLoS Pathog.* 8: e1002839.
10. Coffman, R. L., A. Sher, and R. A. Seder. 2010. Vaccine adjuvants: putting innate immunity to work. *Immunity* 33: 492–503.
11. He, S., X. Mao, H. Sun, T. Shirakawa, H. Zhang, and X. Wang. 2015. Potential therapeutic targets in the process of nucleic acid recognition: opportunities and challenges. *Trends Pharmacol. Sci.* 36: 51–64.
12. Moyer, T. J., A. C. Zmolek, and D. J. Irvine. 2016. Beyond antigens and adjuvants: formulating future vaccines. *J. Clin. Invest.* 126: 799–808.
13. Lee, S., and M. T. Nguyen. 2015. Recent advances of vaccine adjuvants for infectious diseases. *Immune Netw.* 15: 51–57.
14. Pulendran, B., P. S. Arunachalam, and D. T. O'Hagan. 2021. Emerging concepts in the science of vaccine adjuvants. *Nat. Rev. Drug Discov.* 20: 454–475.
15. Reed, S. G., M. Tomai, and M. J. Gale, Jr. 2020. New horizons in adjuvants for vaccine development. *Curr. Opin. Immunol.* 65: 97–101.
16. Ziegler, A., C. Soldner, S. Lienenklaus, J. Spanier, S. Trittel, P. Riese, T. Kramps, S. Weiss, R. Heidenreich, E. Jasny, et al. 2017. A new RNA-based adjuvant enhances virus-specific vaccine responses by locally triggering TLR- and RLH-dependent effects. *J. Immunol.* 198: 1595–1605.
17. Beljanski, V., C. Chiang, G. A. Kirchenbaum, D. Olagnier, C. E. Bloom, T. Wong, E. K. Haddad, L. Trautmann, T. M. Ross, and J. Hiscott. 2015. Enhanced influenza virus-like particle vaccination with a structurally optimized RIG-I agonist as adjuvant. *J. Virol.* 89: 10612–10624.
18. Hochheiser, K., M. Klein, C. Gottschalk, F. Hoss, S. Scheu, C. Coch, G. Hartmann, and C. Kurts. 2016. Cutting edge: the RIG-I ligand 3pRNA potently improves CTL cross-priming and facilitates antiviral vaccination. *J. Immunol.* 196: 2439–2443.
19. Kulkarni, R. R., M. A. Rasheed, S. K. Bhaumik, P. Ranjan, W. Cao, C. Davis, K. Marisetti, S. Thomas, S. Gangappa, S. Sambhara, and K. Murali-Krishna. 2014. Activation of the RIG-I pathway during influenza vaccination enhances the germinal center reaction, promotes T follicular helper cell induction, and provides a dose-sparing effect and protective immunity. *J. Virol.* 88: 13990–14001.
20. Mercado-López, X., C. R. Cotter, W. K. Kim, Y. Sun, L. Muñoz, K. Tapia, and C. B. López. 2013. Highly immunostimulatory RNA derived from a Sendai virus defective viral genome. *Vaccine* 31: 5713–5721.
21. Linehan, M. M., T. H. Dickey, E. S. Molinari, M. E. Fitzgerald, O. Potapova, A. Iwasaki, and A. M. Pyle. 2018. A minimal RNA ligand for potent RIG-I activation in living mice. *Sci. Adv.* 4: e1701854.
22. Bedard, K. M., M. L. Wang, S. C. Proll, Y. M. Loo, M. G. Katze, M. Gale, Jr., and S. P. Iadonato. 2012. Isoflavone agonists of IRF-3 dependent signaling have antiviral activity against RNA viruses. *J. Virol.* 86: 7334–7344.
23. Pattabhi, S., C. R. Wilkins, R. Dong, M. L. Knoll, J. Posakony, S. Kaiser, C. E. Mire, M. L. Wang, R. C. Ireton, T. W. Geisbert, et al. 2015. Targeting innate immunity for antiviral therapy through small molecule agonists of the RLR pathway. *J. Virol.* 90: 2372–2387.
24. Probst, P., J. B. Grigg, M. Wang, E. Muñoz, Y. M. Loo, R. C. Ireton, M. Gale, Jr., S. P. Iadonato, and K. M. Bedard. 2017. A small-molecule IRF3 agonist functions as an influenza vaccine adjuvant by modulating the antiviral immune response. *Vaccine* 35: 1964–1971.
25. Szretter, K. J., A. L. Balish, and J. M. Katz. 2006. Influenza: propagation, quantification, and storage. *Curr. Protoc. Microbiol.* 3: 15G.1.1–15G.1.22.
26. Wong, S. S., and R. J. Webby. 2013. Traditional and new influenza vaccines. *Clin. Microbiol. Rev.* 26: 476–492.
27. Krammer, F., and P. Palese. 2015. Advances in the development of influenza virus vaccines. [Published erratum appears in 2015 *Nat. Rev. Drug Discov.* 14: 294.] *Nat. Rev. Drug Discov.* 14: 167–182.
28. Manicassamy, B., R. A. Medina, R. Hai, T. Tsibane, S. Stertz, E. Nistal-Villán, P. Palese, C. F. Basler, and A. García-Sastre. 2010. Protection of mice against lethal challenge with 2009 H1N1 influenza A virus by 1918-like and classical swine H1N1 based vaccines. *PLoS Pathog.* 6: e1000745.
29. Liu, H. M., Y. M. Loo, S. M. Horner, G. A. Zornetzer, M. G. Katze, and M. Gale, Jr. 2012. The mitochondrial targeting chaperone 14-3-3ε regulates a RIG-I translocon that mediates membrane association and innate antiviral immunity. *Cell Host Microbe* 11: 528–537.
30. Kaufmann, L., M. Syedbasha, D. Vogt, Y. Hollenstein, J. Hartmann, J. E. Linnik, and A. Egli. 2017. An optimized hemagglutination inhibition (HI) assay to quantify influenza-specific antibody titers. *J. Vis. Exp.* 130: 55833.
31. Schneider, C. A., W. S. Rasband, and K. W. Eliceiri. 2012. NIH Image to ImageJ: 25 years of image analysis. *Nat. Methods* 9: 671–675.
32. Gentleman, R. C., V. J. Carey, D. M. Bates, B. Bolstad, M. Dettling, S. Dudoit, B. Ellis, L. Gautier, Y. Ge, J. Gentry, et al. 2004. Bioconductor: open software development for computational biology and bioinformatics. *Genome Biol.* 5: R80.
33. Smyth, G. K. 2004. Linear models and empirical bayes methods for assessing differential expression in microarray experiments. *Stat. Appl. Genet. Mol. Biol.* 3: Article3.
34. Huang, D. W., B. T. Sherman, Q. Tan, J. R. Collins, W. G. Alvord, J. Roayaei, R. Stephens, M. W. Baseler, H. C. Lane, and R. A. Lempicki. 2007. The DAVID Gene Functional Classification Tool: a novel biological module-centric algorithm to functionally analyze large gene lists. *Genome Biol.* 8: R183.
35. Huang, D. W., B. T. Sherman, Q. Tan, J. Kir, D. Liu, D. Bryant, Y. Guo, R. Stephens, M. W. Baseler, H. C. Lane, and R. A. Lempicki. 2007. DAVID Bioinformatics Resources: expanded annotation database and novel algorithms to better extract biology from large gene lists. *Nucleic Acids Res.* 35 (Suppl. 2): W169–W175.
36. Chen, E. Y., C. M. Tan, Y. Kou, Q. Duan, Z. Wang, G. V. Meirelles, N. R. Clark, and A. Ma'ayan. 2013. Enrichr: interactive and collaborative HTML5 gene list enrichment analysis tool. *BMC Bioinformatics* 14: 128.
37. Breuer, K., A. K. Foroushani, M. R. Laird, C. Chen, A. Sribnaia, R. Lo, G. L. Winsor, R. E. Hancock, F. S. Brinkman, and D. J. Lynn. 2013. InnateDB: systems biology of innate immunity and beyond–recent updates and continuing curation. *Nucleic Acids Res.* 41(D1): D1228–D1233.
38. Edgar, R., M. Domrachev, and A. E. Lash. 2002. Gene Expression Omnibus: NCBI gene expression and hybridization array data repository. *Nucleic Acids Res.* 30: 207–210.
39. Herr, W., J. Schneider, A. W. Lohse, K. H. Meyer zum Büschenfelde, and T. Wölfel. 1996. Detection and quantification of blood-derived CD8+ T lymphocytes secreting tumor necrosis factor alpha in response to HLA-A2.1-binding melanoma and viral peptide antigens. *J. Immunol. Methods* 191: 131–142.
40. Jing, Y. Y., Z. P. Han, K. Sun, S. S. Zhang, J. Hou, Y. Liu, R. Li, L. Gao, X. Zhao, Q. D. Zhao, et al. 2012. Toll-like receptor 4 signaling promotes epithelial-mesenchymal transition in human hepatocellular carcinoma induced by lipopolysaccharide. *BMC Med.* 10: 98.
41. Ding, Q., X. Cao, J. Lu, B. Huang, Y. J. Liu, N. Kato, H. B. Shu, and J. Zhong. 2013. Hepatitis C virus NS4B blocks the interaction of STING and TBK1 to evade host innate immunity. *J. Hepatol.* 59: 52–58.
42. Sun, W., Y. Li, L. Chen, H. Chen, F. You, X. Zhou, Y. Zhou, Z. Zhai, D. Chen, and Z. Jiang. 2009. ERIS, an endoplasmic reticulum IFN stimulator, activates innate immune signaling through dimerization. *Proc. Natl. Acad. Sci. USA* 106: 8653–8658.
43. Zhong, B., Y. Yang, S. Li, Y. Y. Wang, Y. Li, F. Diao, C. Lei, X. He, L. Zhang, P. Tien, and H. B. Shu. 2008. The adaptor protein MITA links virus-sensing receptors to IRF3 transcription factor activation. *Immunity* 29: 538–550.
44. Li, K., Z. Chen, N. Kato, M. Gale, Jr., and S. M. Lemon. 2005. Distinct poly(I-C) and virus-activated signaling pathways leading to interferon-beta production in hepatocytes. *J. Biol. Chem.* 280: 16739–16747.
45. Chow, K. T., M. Gale, Jr., and Y. M. Loo. 2018. RIG-I and other RNA sensors in antiviral immunity. *Annu. Rev. Immunol.* 36: 667–694.
46. Ng, C. S., H. Kato, and T. Fujita. 2012. Recognition of viruses in the cytoplasm by RLRs and other helicases–how conformational changes, mitochondrial dynamics and ubiquitination control innate immune responses. *Int. Immunol.* 24: 739–749.
47. Chiang, C., and M. U. Gack. 2017. Post-translational control of intracellular pathogen sensing pathways. *Trends Immunol.* 38: 39–52.
48. Cadena, C., S. Ahmad, A. Xavier, J. Willemsen, S. Park, J. W. Park, S. W. Oh, T. Fujita, F. Hou, M. Binder, and S. Hur. 2019. Ubiquitin-dependent and -independent roles of E3 ligase RIPLET in innate immunity. *Cell* 177: 1187–1200.e16.
49. Lu, H., N. Lu, L. Weng, B. Yuan, Y. J. Liu, and Z. Zhang. 2014. DHX15 senses double-stranded RNA in myeloid dendritic cells. *J. Immunol.* 193: 1364–1372.
50. Mosallanejad, K., Y. Sekine, S. Ishikura-Kinoshita, K. Kumagai, T. Nagano, A. Matsuzawa, K. Takeda, I. Naguro, and H. Ichijo. 2014. The DEAH-box RNA helicase DHX15 activates NF-κB and MAPK signaling downstream of MAVS during antiviral responses. *Sci. Signal.* 7: ra40.
51. Pattabhi, S., M. L. Knoll, M. J. Gale, Jr., and Y.-M. Loo. 2019. DHX15 is a coreceptor for RLR signaling that promotes antiviral defense against RNA virus infection. *J. Interferon Cytokine Res.* 39: 331–346.
52. Wang, P., S. Zhu, L. Yang, S. Cui, W. Pan, R. Jackson, Y. Zheng, A. Rongvaux, Q. Sun, G. Yang, et al. 2015. Nlrp6 regulates intestinal antiviral innate immunity. *Science* 350: 826–830.
53. Fullam, A., and M. Schröder. 2013. DExD/H-box RNA helicases as mediators of antiviral innate immunity and essential host factors for viral replication. *Biochim. Biophys. Acta* 1829: 854–865.
54. Garbelli, A., S. Beermann, G. Di Cicco, U. Dietrich, and G. Maga. 2011. A motif unique to the human DEAD-box protein DDX3 is important for nucleic acid binding, ATP hydrolysis, RNA/DNA unwinding and HIV-1 replication. *PLoS One* 6: e19810.
55. Gu, L., A. Fullam, R. Brennan, and M. Schröder. 2013. Human DEAD box helicase 3 couples IκB kinase ε to interferon regulatory factor 3 activation. *Mol. Cell. Biol.* 33: 2004–2015.
56. Alanio, C., F. Lemaitre, H. K. Law, M. Hasan, and M. L. Albert. 2010. Enumeration of human antigen-specific naive CD8+ T cells reveals conserved precursor frequencies. *Blood* 115: 3718–3725.
57. Pittet, M. J., D. Valmori, P. R. Dunbar, D. E. Speiser, D. Liénard, F. Lejeune, K. Fleischhauer, V. Cerundolo, J. C. Cerottini, and P. Romero. 1999. High frequencies of naive Melan-A/MART-1-specific CD8(+) T cells in a large proportion of human histocompatibility leukocyte antigen (HLA)-A2 individuals. *J. Exp. Med.* 190: 705–716.
58. Wölfl, M., and P. D. Greenberg. 2014. Antigen-specific activation and cytokine-facilitated expansion of naive, human CD8+ T cells. *Nat. Protoc.* 9: 950–966.